



# Complexes of cupric ion and tartaric acid enhanced calcium peroxide Fenton-like reaction for metronidazole degradation

Shiyu Pan, Bo Cao, Deling Yuan\*, Tifeng Jiao, Qingrui Zhang, Shoufeng Tang\*

State Key Laboratory of Metastable Materials Science and Technology, Hebei Key Laboratory of Heavy Metal Deep-Remediation in Water and Resource Reuse, School of Environmental and Chemical Engineering, Yanshan University, Qinhuangdao 066004, China

## ARTICLE INFO

### Article history:

Received 14 June 2023

Revised 7 September 2023

Accepted 9 October 2023

Available online 10 October 2023

### Keywords:

Cupric ion

Tartaric acid

Complexation

Calcium peroxide

Metronidazole removal

## ABSTRACT

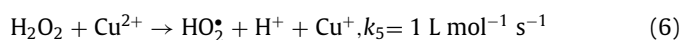
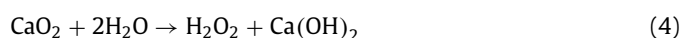
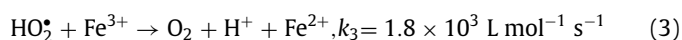
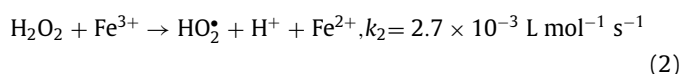
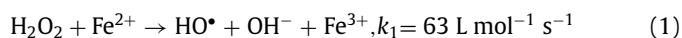
To surmount the obstacles of traditional Fenton method and synchronously utilize  $\text{Cu}^{2+}$  and polyphenol in water, an improved Fenton-like reaction applying calcium peroxide ( $\text{CaO}_2$ ) as  $\text{H}_2\text{O}_2$  source and regulating by the complex of  $\text{Cu}^{2+}$ -tartaric acid (TA, a representative of polyphenol) was constructed. A typical antibiotic, metronidazole (MTZ) could be effectively eliminated by the  $\text{Cu}^{2+}$ /TA/ $\text{CaO}_2$  system, and the optimized parameters were as follows: 0.1 mmol/L  $\text{Cu}^{2+}$ , 2 mmol/L TA, 2 mmol/L  $\text{CaO}_2$ , and initial pH 5. UV spectrum confirmed the formation of  $\text{Cu}^{2+}$ -TA complex, which promoted the  $\text{Cu}^{2+}$ / $\text{Cu}^+$  circulation through decreasing the  $\text{Cu}^{2+}$ / $\text{Cu}^+$  couple redox potential, which further enhanced the  $\text{H}_2\text{O}_2$  decomposition and the formation of reactive species. Hydroxyl radical was dominant for MTZ degradation, followed by oxygen and superoxide radical. The degradation intermediates of MTZ were detected and their evolution way was speculated. Furthermore, the ternary process showed a wide pH tolerance (3–8) for removing MTZ and broad applicability for eliminating other dyes and antibiotics. This work provided a reference for Cu-based Fenton-like strategy for organic wastewater settlement.

© 2024 Published by Elsevier B.V. on behalf of Chinese Chemical Society and Institute of Materia Medica, Chinese Academy of Medical Sciences.

Advanced oxidation processes (AOPs) have been universally recognized strategy for the treatment of organic contaminants [1]. The traditional Fenton can non-selectively remove the organics by hydroxyl radical ( $\text{HO}^\bullet$ ), which is generated from the ferrous ion ( $\text{Fe}^{2+}$ ) activated hydrogen peroxide ( $\text{H}_2\text{O}_2$ ) process at acidic conditions (Eqs. 1–3) [2]. Nevertheless, there are a few inherent limitations for the Fenton reaction, including the narrow application range of pH [3,4], the slow ferric ion ( $\text{Fe}^{3+}$ )/ $\text{Fe}^{2+}$  circulation rate [5,6], and the instability of  $\text{H}_2\text{O}_2$  [7]. As a solid oxidant, calcium peroxide ( $\text{CaO}_2$ ) is easier to store and transport, which can slowly release  $\text{H}_2\text{O}_2$  (Eq. 4) [8]. The decomposition rate of  $\text{CaO}_2$  could be controlled by adjusting pH, which could avoid the disproportionation of  $\text{H}_2\text{O}_2$  [9]. Therefore,  $\text{CaO}_2$  is considered as an effective substitute for  $\text{H}_2\text{O}_2$  [10].

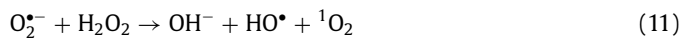
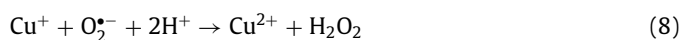
On the other side, as another common transition metal, cupric ion ( $\text{Cu}^{2+}$ ) is ubiquitous in multiple waterbodies [11,12].  $\text{Cu}^{2+}$  has a larger solubility ( $K_{\text{sp}} \text{Cu}(\text{OH})_2 = 4.8 \times 10^{-20}$ ) than that of  $\text{Fe}^{3+}$  ( $K_{\text{sp}} \text{Fe}(\text{OH})_3 = 2.8 \times 10^{-39}$ ) [13], and the circulation of  $\text{Cu}^{2+}$ /cuprous ion ( $\text{Cu}^+$ ) is easier than that of  $\text{Fe}^{3+}$ / $\text{Fe}^{2+}$  due to the lower standard potential ( $E^0(\text{Fe}^{3+}/\text{Fe}^{2+}) = 0.77 \text{ V vs. SHE}$ ,  $E^0(\text{Cu}^{2+}/\text{Cu}^+) = 0.17 \text{ V vs. SHE}$ ) [14], which means the Cu-based Fen-

ton process is superior with a greater pH tolerance and better catalytic activity (Eqs. 5 and 6) than the Fe-based Fenton method [11]. Therefore, if the  $\text{Cu}^{2+}$  existed in water matrix can be *in-situ* used to activate Fenton/Fenton-like reactions, which could put forward to the practicality of the homogeneous Cu-based Fenton-like system. However, similar to the conventional Fenton reaction, the slow reduction of  $\text{Cu}^{2+}$  to  $\text{Cu}^+$  ( $k = 1 \text{ L mol}^{-1} \text{ s}^{-1}$ ) remains the rate-limiting step [15,16]. Thus, exploring a skill to accelerate the  $\text{Cu}^{2+}$ / $\text{Cu}^+$  circulation is imperative for promoting this Fenton-like reaction.



\* Corresponding authors.

E-mail addresses: yuandl@ysu.edu.cn (D. Yuan), tangshf@ysu.edu.cn (S. Tang).



The complexation of  $\text{Cu}^{2+}$  with organic ligands could alter the activity of  $\text{Cu}^{2+}/\text{Cu}^+$  couple, and stabilize Cu ions in terms of electronic property and steric effect [12]. Moreover, some  $\text{Cu}^{2+}$  complexes could efficiently trigger  $\text{H}_2\text{O}_2$  or persulfates to produce radicals, for degrading diverse organic pollutants [17]. However, some organic ligands, such as ethylenediaminetetraacetic acid [18,19], pyridine [17], and ethylenediamine [20], they are themselves contaminants, which not only increase the amount of organic matter and bring secondary pollution, but also quench free radicals by their self-degradation effect [21]. Hence, searching an environmentally friendly organic ligand is the key for improving homogeneous Cu-based Fenton-like system.

Plant-derived polyphenols belong to natural organic matter (NOM) and also low-molecular-weight organic acids, which are commonly found in the natural environments, including water [11,22]. The hydroxyl groups of polyphenols have the property of strong electron donor [23], which could mediate the  $\text{Cu}^{2+}/\text{Cu}^+$  cycle and then reduce  $\text{Cu}^{2+}$  to  $\text{Cu}^+$  [11,24], triggering a series of chain reactions (Eqs. 5-11) to generate  $\text{HO}^\bullet$ , superoxide ( $\text{O}_2^{\cdot-}$ ), and singlet oxygen ( ${}^1\text{O}_2$ ) [25,26]. Tartaric acid (TA) is a typical polyphenol, comes from grape and tamarind [10,27], which could be strongly complexed with Fe ions and regulate their redox cycling [28,29]. Nevertheless, there has been an obvious knowledge gap in the function of TA complexed with Cu ions for Fenton/Fenton-like processes.

Based on above, the *in-situ* simultaneous utilizations of  $\text{Cu}^{2+}$  and NOM in water might realize the most efficient implementation for Fenton/Fenton-like reactions [30]. Thus, in this study, the effectiveness of  $\text{Cu}^{2+}$ -TA complex for catalyzing  $\text{CaO}_2$ -based Fenton-like system was verified for metronidazole (MTZ) elimination. The systematical study centered around the followings: (1) Determine the influences of key factors (the dosages of  $\text{Cu}^{2+}$ , TA, and  $\text{CaO}_2$ , and pH) of the ternary processes; (2) investigate the catalytic function of  $\text{Cu}^{2+}$ -TA complex; (3) explore the evolution and contribution of reactive oxygen species (ROS) during this Cu-based Fenton-like reaction.

The specific chemicals of the work were recorded in Text S1 (Supporting information). The batch experiment was conducted in a 150 mL glass vessel under electromagnetic stirring at room-temperature. The desired concentration of MTZ was configured with phosphate buffer, which fixed the initial pH of the reaction solution. TA and cupric chloride ( $\text{CuCl}_2$ ) were successively added into 100 mL of MTZ solution, the experiment was triggered once added the desired concentration of  $\text{CaO}_2$ . All the tests were conducted at least in twice. MTZ concentration was detected through UV spectroscopy at 320 nm [13,31]. *Tert*-butyl alcohol (TBA), *L*-Histidine (*L*-His), and *p*-benzoquinone (*p*-BQ) were selected as the ROS scavenger, and the generation of ROS was detected by electron spin resonance technique (ESR). The concentration of  $\text{H}_2\text{O}_2$  was determined by potassium titanium oxalate colorimetry [13]. The content of Cu ions was measured by neocuproine spectrophotometry [32]. Electro-chemical workstation was applied to conduct the cyclic voltammetry measurement [13].

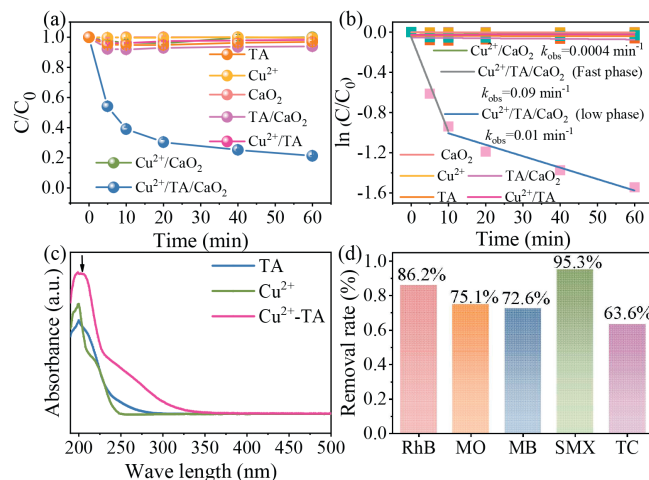


**Fig. 1.** (a) Elimination for MTZ in different systems and (b) corresponding pseudo-first-order kinetic rate constant. (c) UV-vis absorption spectra of  $\text{Cu}^{2+}$ , TA, and  $\text{Cu}^{2+}$ -TA. (d) Degradation of different organic contaminants in  $\text{Cu}^{2+}/\text{TA}/\text{CaO}_2$  system. Experimental condition:  $[\text{Cu}^{2+}]_0 = 0.1 \text{ mmol/L}$ ,  $[\text{TA}]_0 = 2 \text{ mmol/L}$ ,  $[\text{CaO}_2]_0 = 2 \text{ mmol/L}$ ,  $\text{pH}_0 = 5$ ,  $[\text{MTZ}] = [\text{MB}] = [\text{MO}] = [\text{RhB}] = [\text{SMX}] = [\text{TC}] = 5 \text{ mg/L}$ .

MTZ decomposed intermediates were determined by high performance liquid chromatography-mass spectrometry (HPLC-MS). The detailed analysis and operation were listed in Text S2 (Supporting information).

The enhancement effect of TA on  $\text{Cu}^{2+}/\text{CaO}_2$  was evaluated by comparing the degradation efficiencies of MTZ in diverse processes. Fig. 1a shows the removal of MTZ was negligible in  $\text{Cu}^{2+}/\text{CaO}_2$  after 60 min. Nevertheless, the elimination of MTZ augmented to 78.7% in the  $\text{Cu}^{2+}/\text{TA}/\text{CaO}_2$  system. The apparent rate constant ( $k_{\text{obs}}$ ) of MTZ degradation in  $\text{Cu}^{2+}/\text{TA}/\text{CaO}_2$  process was 225 times higher than that in  $\text{Cu}^{2+}/\text{CaO}_2$  in the first 10 min, and 25 times higher in the following 50 min reaction (Fig. 1b). The decrease of  $k_{\text{obs}}$  during the following 50 min might be ascribed to the quickly falling  $\text{H}_2\text{O}_2$ . Furthermore, the insignificant degradation of MTZ was observed in  $\text{TA}/\text{CaO}_2$  and  $\text{Cu}^{2+}/\text{TA}$  systems, which indicated that TA could not activate  $\text{CaO}_2$  directly, and  $\text{CaO}_2$  was the motivity of MTZ removal [33]. UV-vis spectrum was employed to verify the formation of  $\text{Cu}^{2+}$ -TA complex. As depicted in Fig. 1c, compared with the spectra of  $\text{Cu}^{2+}$  and sole TA, an emerging absorption peak was appeared around 213 nm in the mixed sample of  $\text{Cu}^{2+}$  and TA, which testified the production of  $\text{Cu}^{2+}$ -TA metal organic ligand. TA might serve as the chelating agent to mediate the redox potential of Cu ions and promote the generation of ROS [18], therefore enhancing the performance of the  $\text{Cu}^{2+}/\text{CaO}_2$  system.

Besides, Fig. 1d shows the  $\text{Cu}^{2+}/\text{TA}/\text{CaO}_2$  process also had the remarkable capability for other contaminants removal, including rhodamine b (RhB), sulfamethoxazole (SMX), methyl orange (MO), tetracycline (TC), and methylene blue (MB). Furthermore, Fig. S1 (Supporting information) shows that 34.6% of chemical oxygen demand (COD) removal ratio was reached for domestic sewage by the synergistic process after 180 min reaction. Besides, the total organic carbon (TOC) removal achieved 20.2% after 180 min (Fig. S2 in Supporting information). Thus, the ternary system possessed an extensive applicability and actual potential for removing organic pollutants in wastewater.

The influences of specific reaction parameters on the elimination of MTZ in the  $\text{Cu}^{2+}/\text{TA}/\text{CaO}_2$  system were systematically investigated, including  $\text{Cu}^{2+}$  dosage (Fig. 2a), TA dosage (Fig. 2b), and  $\text{CaO}_2$  concentration (Fig. 2c). The results manifested that  $\text{Cu}^{2+}$ , TA, and  $\text{CaO}_2$  were all indispensable factors, the absence of any one of them would seriously affect the degradation of MTZ. Furthermore, the higher dosages of  $\text{Cu}^{2+}$  and  $\text{CaO}_2$  would accelerate the

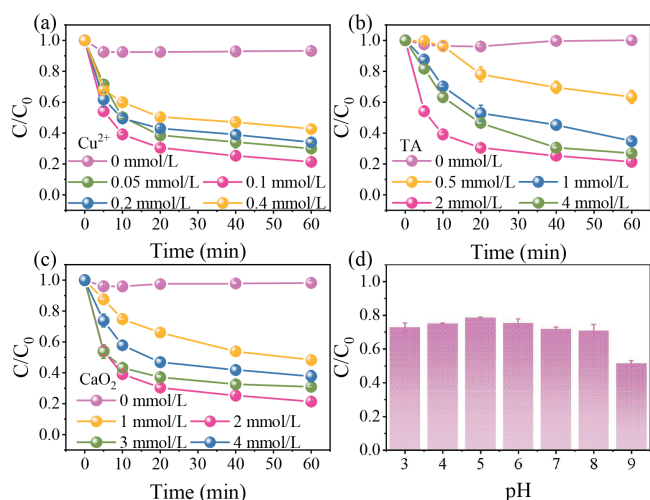


**Fig. 2.** Influences of (a)  $\text{Cu}^{2+}$ , (b) TA, (c)  $\text{CaO}_2$ , and (d) pH on MTZ degradation in  $\text{Cu}^{2+}/\text{TA}/\text{CaO}_2$  system. Experimental condition:  $[\text{Cu}^{2+}]_0 = 0.05\text{--}0.4$  mmol/L,  $[\text{TA}]_0 = 0.5\text{--}4$  mmol/L,  $[\text{CaO}_2]_0 = 1\text{--}4$  mmol/L, pH<sub>0</sub> 3–9,  $[\text{MTZ}] = 5$  mg/L.

generation of  $\text{HO}^\bullet$  to trigger the self-quenching reaction (Eq. 9) to restrain the elimination of MTZ. TA as an organic compound would compete  $\text{HO}^\bullet$  with MTZ, hence the excess TA also hindered the removal of MTZ. Therefore, after the comprehensive investigation, the optimal experimental dosages were as follows: 0.1 mmol/L  $\text{Cu}^{2+}$ , 2 mmol/L TA, and 2 mmol/L  $\text{CaO}_2$ . Moreover, the ternary process indicated a wide pH tolerance, as described in Fig. 2d, MTZ could be eliminated efficiently as the pH values increased from 3 to 8. Above results proved the benign catalytic ability of  $\text{Cu}^{2+}$ -TA complex.

Moreover, the resistant ability for common anions (chloridion ( $\text{Cl}^-$ ), sulfate ion ( $\text{SO}_4^{2-}$ ), nitrate ion ( $\text{NO}_3^-$ ), and bicarbonate ion ( $\text{HCO}_3^-$ )) on the  $\text{Cu}^{2+}/\text{TA}/\text{CaO}_2$  system was investigated (Fig. S3 in Supporting information). The complexing system represented a great resistant ability for different anions expect  $\text{HCO}_3^-$ . Carbonate radical anion ( $\text{CO}_3^{\cdot-}$ ) with lower redox potential (1.59 V) would be generated by  $\text{HCO}_3^-$  quenching  $\text{HO}^\bullet$  (Eqs. 12–14), which would inhibit the degradation of MTZ [34,35].



To investigate the role of TA in the enhanced  $\text{Cu}^{2+}/\text{CaO}_2$  process, the change of  $\text{Cu}^{2+}/\text{Cu}^+$  cycle and  $\text{H}_2\text{O}_2$  concentration during the reaction were compared in  $\text{Cu}^{2+}/\text{CaO}_2$  and  $\text{Cu}^{2+}/\text{TA}/\text{CaO}_2$ . As displayed in Fig. 3a, 0.19 mg/L of  $\text{Cu}^+$  was produced in  $\text{Cu}^{2+}/\text{CaO}_2$  system, the weak reduction of  $\text{Cu}^{2+}$  to  $\text{Cu}^+$  might be the reason for hindering MTZ degradation. However, the  $\text{Cu}^{2+}$  was almost completely converted into  $\text{Cu}^+$  in the present of TA (Fig. 3b), which testified that the  $\text{Cu}^{2+}$ -TA complex could effectually accelerate the reduction of  $\text{Cu}^{2+}$ . In addition, the consumption of  $\text{H}_2\text{O}_2$  in different systems was also investigated (Fig. 3c). Firstly, 5.88 mmol/L  $\text{H}_2\text{O}_2$  could be released by  $\text{CaO}_2$  alone, and only 0.2 mmol/L of  $\text{H}_2\text{O}_2$  was decomposed in  $\text{Cu}^{2+}/\text{CaO}_2$ . In  $\text{Cu}^{2+}/\text{TA}/\text{CaO}_2$  system,  $\text{H}_2\text{O}_2$  could be consumed rapidly, and the concentration of  $\text{H}_2\text{O}_2$  was declined from 5.82 mmol/L to 0.05 mmol/L after 60 min. These results proved that the  $\text{Cu}^{2+}$ -TA complex could availably promote the disintegration of  $\text{H}_2\text{O}_2$ .

To demonstrate the redox ability of  $\text{Cu}^{2+}$ -TA complex, the cyclic voltammetry (CV) was conducted in the  $\text{Cu}^{2+}$  system with or without TA. As shown in Fig. 3d, the peaks of  $A_1$  and  $A_2$  were owed to

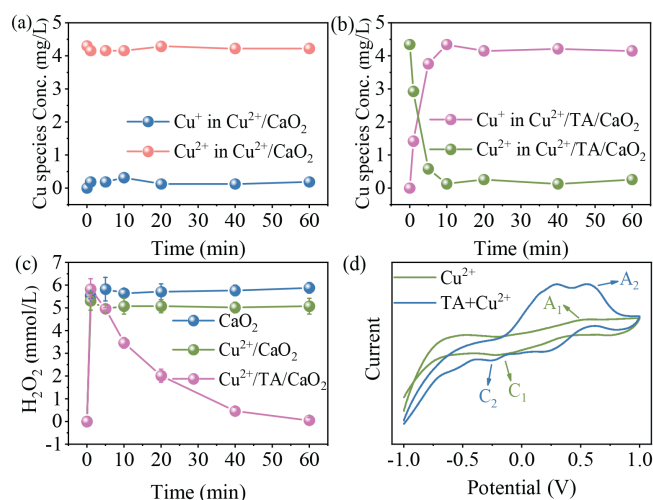
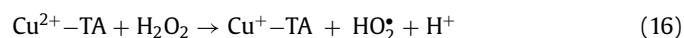
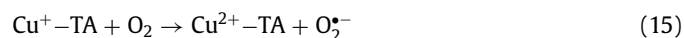


**Fig. 3.** Variation of  $\text{Cu}^{2+}$  and  $\text{Cu}^+$  concentration in  $\text{Cu}^{2+}/\text{CaO}_2$  (a) and  $\text{Cu}^{2+}/\text{TA}/\text{CaO}_2$  systems (b). (c) Change of  $\text{H}_2\text{O}_2$  concentration in different systems. (d) CV of  $\text{Cu}^{2+}$ -TA. Experimental condition:  $[\text{Cu}^{2+}]_0 = 0.1$  mmol/L,  $[\text{TA}]_0 = 2$  mmol/L,  $[\text{CaO}_2]_0 = 2$  mmol/L, pH<sub>0</sub> 5,  $[\text{MTZ}] = 5$  mg/L.

the oxidation of  $\text{Cu}^+$  to  $\text{Cu}^{2+}$ , while  $C_1$  and  $C_2$  were the reducing peaks of  $\text{Cu}^{2+}$  to  $\text{Cu}^+$  [13]. The higher peak potential in the mixed  $\text{Cu}^{2+}$  and TA solution ( $A_2$ ,  $C_2$ ) indicated that the  $\text{Cu}^{2+}$ -TA complex had the greater redox capacity. Hence, TA chelated with  $\text{Cu}^{2+}$  in the  $\text{Cu}^{2+}/\text{TA}/\text{CaO}_2$  could reduce the  $\text{Cu}^{2+}/\text{Cu}^+$  redox potential to improve the  $\text{Cu}^{2+}/\text{Cu}^+$  cycle, enhancing the  $\text{H}_2\text{O}_2$  disintegration and the ROS production [13].

The primary ROS in the  $\text{Cu}^{2+}/\text{TA}/\text{CaO}_2$  were clarified firstly by quenching experiment. TBA was applied to quench  $\text{HO}^\bullet$  ( $k_{\text{HO}^\bullet, \text{TBA}} = 6 \times 10^8 \text{ L mol}^{-1} \text{ s}^{-1}$ ) [36,37]. As described in Fig. 4a, MTZ removal efficiency significantly declined to 24.2% under 2 mmol/L TBA, indicating that  $\text{HO}^\bullet$  played the dominant role for MTZ elimination. Moreover, *p*-BQ and L-His were selected to suppress  $\text{O}_2^{\cdot-}$  and  $^1\text{O}_2$  ( $k_{\text{O}_2^{\cdot-}, p\text{-BQ}} = (0.9\text{--}1) \times 10^9 \text{ L mol}^{-1} \text{ s}^{-1}$ ,  $k_{^1\text{O}_2, \text{L-His}} = 3.2 \times 10^7 \text{ L mol}^{-1} \text{ s}^{-1}$ ), separately [38–40]. As shown in Figs. 4b and c, the slight quenching effect of *p*-BQ and L-His illustrated that  $\text{O}_2^{\cdot-}$  and  $^1\text{O}_2$  both played the minor role in this system. Utterly, ESR was employed to confirm the existence of ROS. 5,5-dimethyl-1-pyrrolidine-*N*-oxide (DMPO) was used to trap  $\text{HO}^\bullet$  and  $\text{O}_2^{\cdot-}$ , 2,2,6,6-tetramethylpiperidine (TEMP) was employed to capture  $^1\text{O}_2$  [38,41]. As presented in Figs. 4d–f, the typical signals of DMPO- $\text{HO}^\bullet$ , DMPO- $\text{O}_2^{\cdot-}$ , and TEMP- $^1\text{O}_2$  adducts were detected in both processes with and without TA. Of note, the signal intensity of  $\text{Cu}^{2+}/\text{TA}/\text{CaO}_2$  was obviously stronger than that of  $\text{Cu}^{2+}/\text{CaO}_2$ , which affirmed the role of TA on the enhancement of ROS generation in this Cu-based Fenton-like reaction.

The generated  $\text{HO}^\bullet$  exhibited triple roles in this system: (1) contributing to the degradation of MTZ; (2) reacting with the excess  $\text{H}_2\text{O}_2$  to generate the secondary  $\text{O}_2^{\cdot-}$  and  $^1\text{O}_2$  (Eqs. 9–11); (3) attacking the electrophilic TA into the small molecule. Furthermore,  $\text{Cu}^+$ -TA also reacted with  $\text{O}_2$  to promote the production of  $\text{O}_2^{\cdot-}$  (Eq. (15)), and the generated  $\text{Cu}^{2+}$ -TA reacted with the excess  $\text{H}_2\text{O}_2$  to sustain the  $\text{Cu}^{2+}/\text{Cu}^+$  cycle (Eq. 16) [42]. However,  $\text{O}_2^{\cdot-}$  and  $^1\text{O}_2$  could not effectively remove MTZ due to the low oxidation capacity ( $k_{\text{O}_2^{\cdot-}, \text{MTZ}} = 0 \text{ L mol}^{-1} \text{ s}^{-1}$ ,  $k_{^1\text{O}_2, \text{MTZ}} = 1.5 \times 10^8 \text{ L mol}^{-1} \text{ s}^{-1}$ ), so  $\text{HO}^\bullet$  was the dominant ROS for MTZ elimination ( $k_{\text{HO}^\bullet, \text{MTZ}} = 6 \times 10^9 \text{ L mol}^{-1} \text{ s}^{-1}$ ) in the ternary system, followed by  $^1\text{O}_2$  and  $\text{O}_2^{\cdot-}$  [43,44].



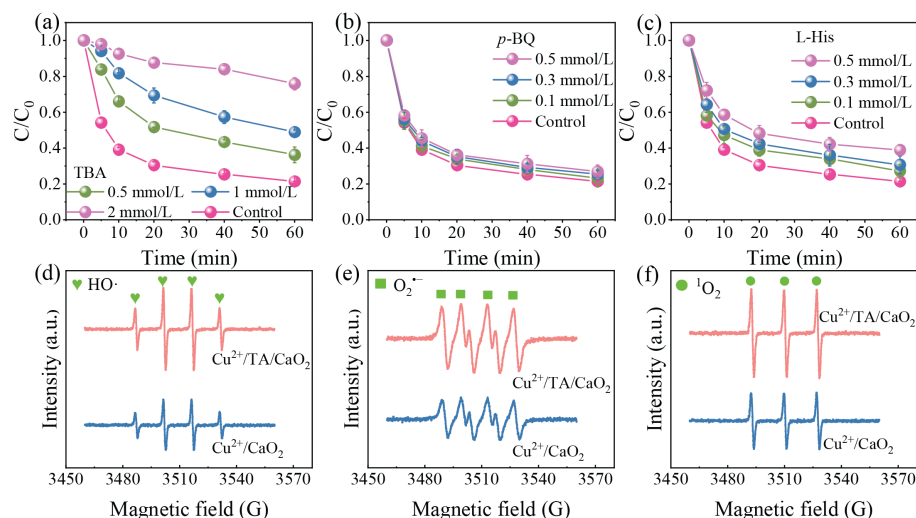


**Fig. 4.** Influences of (a) TBA, (b) *p*-BQ, and (c) L-His on MTZ degradation in  $\text{Cu}^{2+}/\text{TA}/\text{CaO}_2$  system. EPR spectra of (d) DMPO- $\text{HO}^\bullet$  adduct, (e) DMPO- $\text{O}_2^{\bullet-}$  adduct, and (f) TEMP- $^1\text{O}_2$  adduct in both systems. Experimental condition:  $[\text{Cu}^{2+}]_0 = 0.1 \text{ mmol/L}$ ,  $[\text{TA}]_0 = 2 \text{ mmol/L}$ ,  $[\text{CaO}_2]_0 = 2 \text{ mmol/L}$ ,  $[\text{TBA}]_0 = 0.5\text{--}2 \text{ mmol/L}$ ,  $[\text{p-BQ}]_0 = [\text{L-His}]_0 = 0.1\text{--}0.5 \text{ mmol/L}$ ,  $\text{pH}_0 5$ ,  $[\text{MTZ}] = 5 \text{ mg/L}$ .

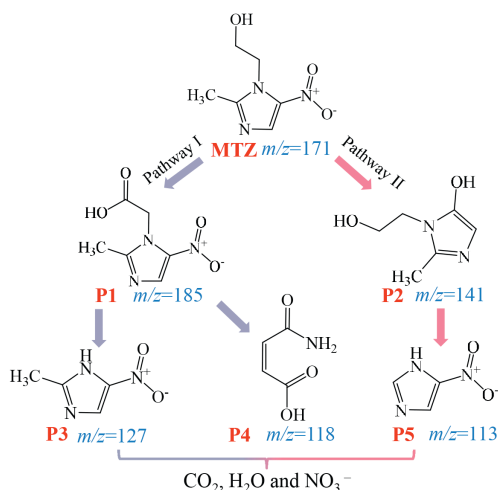
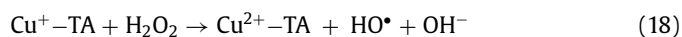


**Fig. 5.** Speculated decomposition pathways of MTZ.

According to the result of HPLC-MS, the possible degradation pathways of MTZ during  $\text{Cu}^{2+}/\text{TA}/\text{CaO}_2$  were proposed. As revealed in Fig. 5, firstly, (2-methyl-5-nitroimidazol-1-yl) acetic acid (**P1**,  $m/z = 185$ ) might be produced by the *N*-ethanol group oxidation of MTZ [45,46]. Next,  $\text{HO}^\bullet$  attacked the *N*-acetic acid group of **P1** and generated 2-methyl-5-nitro-1*H*-imidazole (**P3**,  $m/z = 127$ ) [45,47], or **P1** underwent hydroxylation and ring opening reaction to form 3-carbonyl propylene glycol 2-oleic acid (**P4**,  $m/z = 118$ ) [45,48]. In another pathway, 3-(2-hydroxy-ethyl)-2-methyl-3*H*-imidazole-4-ol (**P2**,  $m/z = 141$ ) was formed by the direct hydroxylation of nitro group [45,49]. The crack of *N*-acetic acid group and nitration reaction were occurred on **P2** to form byproduct **P5** ( $m/z = 113$ ) [50]. In addition, the biotoxicity of MTZ and its elimination byproducts was evaluated by toxicity assessment software, the results demonstrated that the oral rat LD<sub>50</sub> (Fig. S4a in Supporting information) and the developmental toxicity (Fig. S4c in Supporting information) of part intermediates were higher than that of MTZ. However, the bioaccumulation factor (Fig. S4b in Supporting information) and the mutagenicity (Fig. S4d in Supporting information) of the intermediates were all decreased after the treatment of the synergic process. Therefore, the  $\text{Cu}^{2+}/\text{TA}/\text{CaO}_2$  process could decrease the biotoxicity of MTZ to some extent, and appropriate prolonga-

tion of reaction might be required to minimize toxicity in practical treatment.

To sum up, the conceivable mechanism of TA enhanced  $\text{Cu}^{2+}/\text{CaO}_2$  system can be summarized as follows. In the  $\text{Cu}^{2+}/\text{CaO}_2$  system, the sluggish  $\text{Cu}^{2+}/\text{Cu}^+$  cycle hindered the activation of  $\text{H}_2\text{O}_2$  (Eqs. 5 and 6), then hampered the elimination of MTZ (Fig. 1a). Upon the TA addition,  $\text{Cu}^{2+}$  was rapidly complexed with the two hydroxyl groups of TA to form a soluble  $\text{Cu}^{2+}$ -TA complex (Eq. 17, Fig. 1c), which could decrease the redox potential of  $\text{Cu}^{2+}/\text{Cu}^+$  (Fig. 3d). The  $\text{Cu}^{2+}$ -TA could be reduced by  $\text{H}_2\text{O}_2$  to form the reductive  $\text{Cu}^+$ -TA, which could improve the reduction of  $\text{Cu}^{2+}$  (Eq. 16, Fig. 3b) and the activation of  $\text{H}_2\text{O}_2$  (Eq. 18, Fig. 3c) [42]. Next, the production of various ROS was enhanced by the complexation, such as  $\text{HO}^\bullet$ ,  $\text{O}_2^{\bullet-}$ , and  $^1\text{O}_2$  (Figs. 4d–f), and the removal of MTZ was also promoted. Overall,  $\text{Cu}^+$ -TA was the critical species to manipulate this ternary system, and TA served as the electron donor to promote the electron transfer in metal-ligand and enhance the generation of ROS.



In summary, the complexation of  $\text{Cu}^{2+}$  and TA could efficaciously catalyze  $\text{CaO}_2$  oxidation of MTZ in the pH extent of 3–8. The addition of TA could accelerate the regeneration of  $\text{Cu}^+$ , which was driven from the formed ligand of  $\text{Cu}^{2+}$  and TA. Furthermore, the  $\text{Cu}^{2+}$ -TA complex could motivate the  $\text{H}_2\text{O}_2$  disintegration and the ROS production.  $\text{HO}^\bullet$  was proved to be the main ROS for MTZ degradation, followed by  $^1\text{O}_2$  and  $\text{O}_2^{\bullet-}$ . MTZ decomposition pathways mainly included hydroxylation, ring opening, attack on specific group, and nitration reactions. This work proved that TA could be a potential chelating agent to promote Fenton-like reaction for degrading different organic contaminants, which provided a referable method for improving the performance of Cu-based Fenton-like system.

#### Declaration of competing interest

The authors declare that they have no known competing financial interests or personal relationships that could have appeared to influence the work reported in this paper.

## Acknowledgments

We thank the supports from the National Natural Science Foundation of China (No. 51908485), the Central Guidance on Local Science and Technology Development Fund of Hebei Province (No. 226Z3603G), Hebei Province Foundation for Returnees (No. C20210502).

## Supplementary materials

Supplementary material associated with this article can be found, in the online version, at doi:10.1016/j.ccl.2023.109185.

## References

- [1] H. Weng, Y. Yang, C. Zhang, et al., *Chem. Eng. J.* 453 (2023) 139812.
- [2] S. Pan, Z. Zhai, K. Yang, et al., *Sep. Purif. Technol.* 289 (2022) 120806.
- [3] C. Wang, B. Wei, H. Zhu, et al., *Chin. Chem. Lett.* 33 (2022) 3073–3077.
- [4] W. Zheng, Y. Liu, F. Liu, et al., *Water Res.* 223 (2022) 118994.
- [5] W. Hu, M. Yang, Q. Yan, et al., *Chin. Chem. Lett.* 34 (2023) 108109.
- [6] Q. Zhao, C. Wang, P. Wang, *Chin. Chem. Lett.* 33 (2022) 4828–4833.
- [7] S. Tang, E. Zhu, Z. Zhai, et al., *Chemosphere* 319 (2023) 138025.
- [8] D. Yuan, C. Zhang, S. Tang, et al., *Chin. Chem. Lett.* 32 (2021) 3387–3392.
- [9] Y. Zhou, X. Fang, T. Wang, Y. Hu, J. Lu, *Chem. Eng. J.* 313 (2017) 638–645.
- [10] S. Tang, Z. Wang, D. Yuan, et al., *J. Clean. Prod.* 268 (2020) 122253.
- [11] Y. Wang, Y. Wu, Y. Yu, et al., *Water Res.* 186 (2020) 116326.
- [12] J. Chen, X. Zhou, P. Sun, Y. Zhang, C. Huang, *Environ. Sci. Technol.* 53 (2019) 11774–11782.
- [13] Q. Ye, H. Xu, Q. Wang, et al., *J. Hazard. Mater.* 407 (2021) 124351.
- [14] G. Pan, Z. Sun, *Chemosphere* 283 (2021) 131257.
- [15] N. Li, T. Liu, S. Xiao, et al., *J. Hazard. Mater.* 445 (2023) 130536.
- [16] L. Jin, S. You, N. Ren, B. Ding, Y. Liu, *Environ. Sci. Technol.* 56 (2022) 11750–11759.
- [17] J. Li, A.N. Pham, R. Dai, Z. Wang, T.D. Waite, *J. Hazard. Mater.* 392 (2020) 122261.
- [18] A. De Luca, R.F. Dantas, S. Esplugas, *Water Res.* 61 (2014) 232–242.
- [19] A. Gabet, C. Guy, A. Fazli, et al., *Sep. Purif. Technol.* 317 (2023) 123877.
- [20] A. Rastogi, S.R. Al-Abied, D.D. Dionysiou, *Water Res.* 43 (2009) 684–694.
- [21] Y. Xiang, K. Yang, Z. Zhai, et al., *Chem. Eng. J.* 438 (2022) 135656.
- [22] H. Zhou, H. Zhang, Y. He, et al., *Appl. Catal. B.* 286 (2021) 119900.
- [23] Q. Ouyang, F. Kou, N. Zhang, et al., *Chem. Eng. J.* 366 (2019) 514–522.
- [24] Y. Bai, D. Wu, W. Wang, et al., *Environ. Res.* 192 (2021) 110242.
- [25] X. Li, Y. Jia, J. Zhang, et al., *Chin. Chem. Lett.* 33 (2022) 2105–2110.
- [26] D. Yuan, C. Zhang, S. Tang, et al., *Water Res.* 163 (2019) 114861.
- [27] M. Rashidipour, Z. Derikvand, A. Shokrollahi, Z. Mohammadpour, A. Azadbakht, *Arab. J. Chem.* 10 (2017) S3167–S3175.
- [28] P. Villegas-Guzman, S. Giannakis, R.A. Torres-Palma, C. Pulgarin, *Appl. Catal. B.* 205 (2017) 219–227.
- [29] Z. Ouyang, C. Yang, J. He, et al., *Chem. Eng. J.* 402 (2020) 126122.
- [30] T. Pan, Y. Wang, X. Yang, X. Huang, R. Qiu, *Chem. Eng. J.* 384 (2020) 123248.
- [31] Y. Xiang, H. Liu, E. Zhu, et al., *Sep. Purif. Technol.* 295 (2022) 121293.
- [32] X. Zhou, H. Luo, B. Sheng, et al., *J. Hazard. Mater.* 411 (2021) 125050.
- [33] M. Zhao, Y. Xiang, X. Jiao, et al., *Sep. Purif. Technol.* 276 (2021) 119289.
- [34] S. Pan, T. Zhao, H. Liu, et al., *Chem. Eng. J.* 452 (2023) 139245.
- [35] Y. Huang, L. Bu, Y. Wu, et al., *Chem. Eng. J.* 442 (2022) 135995.
- [36] F. Ye, W. Sun, K. Pang, et al., *Chin. Chem. Lett.* 34 (2023) 107755.
- [37] M. Wang, M. Fu, J. Li, et al., *Chin. Chem. Lett.* 35 (2024) 108442.
- [38] Y. Li, H. Dong, J. Xiao, et al., *Chem. Eng. J.* 455 (2023) 140773.
- [39] L. Yang, W. Chen, C. Sheng, et al., *Appl. Surf. Sci.* 549 (2021) 149300.
- [40] Z. Yang, Z. Wang, G. Liang, X. Zhang, X. Xie, *Chem. Eng. J.* 426 (2021) 131777.
- [41] P. Yang, A. Shen, Z. Zhu, et al., *Chem. Eng. J.* 464 (2023) 142724.
- [42] J. Guo, X. Chen, Y. Shi, Y. Lan, C. Qin, *PLoS One* 10 (2015) e0134298.
- [43] L. Gao, Y. Guo, J. Zhan, G. Yu, Y. Wang, *Water Res.* 221 (2022) 118730.
- [44] Y. Guo, J. Long, J. Huang, G. Yu, Y. Wang, *Water Res.* 215 (2022) 118275.
- [45] H. Ren, H. Liu, T. Cui, et al., *Chem. Eng. J.* 431 (2022) 133803.
- [46] S. Tang, H. Liu, E. Zhu, et al., *Sep. Purif. Technol.* 301 (2022) 122056.
- [47] J. Cao, J. Li, W. Chu, W. Cen, *Chem. Eng. J.* 400 (2020) 125813.
- [48] X. Guo, B. Hu, K. Wang, et al., *Chem. Eng. J.* 435 (2022) 132910.
- [49] J. Zeng, J. Liu, W. Su, et al., *J. Water Process. Eng.* 53 (2023) 103733.
- [50] X. Tian, T. Luo, Y. Nie, et al., *Environ. Sci. Technol.* 56 (2022) 5542–5551.